67º congresso 2012 abm
67th abm international congress
ISSN 1516-392X

THREE DIMENSIONAL EFFECTS ON ELASTIC NOTCH TIP STRESS/STRAIN FIELDS IN FINITE-THICKNESS PLATES UNDER TENSION[1]

Rafael Cesar de Oliveira Góes[2]
Jaime Tupiassú Pinho de Castro[3]
Luiz Fernando Martha[4]

Abstract
Three dimensional elastic stress and strain fields around elliptic holes and semi-elliptical notches in finite thickness plates are investigated through 3D finite elements analyses. Significant through-thickness variation of stress and strain concentration factors are identified and compared with 2D solutions. Stress gradients are analyzed in the vicinity of the notch-tip and compared with 2D solutions and with data extracted from literature. Finally, considerations are made on impacts of 3D effects on design of notched pieces.
Key words: Three-dimensional notches; Stress concentration; Notch tip stress fields; Thickness effects.

EFEITOS TRIDIMENSIONAIS EM CAMPOS DE TENSÃO E DEFORMAÇÃO EM TORNO DE ENTALHES EM PLACAS DE ESPESSURA FINITA TRACINADAS

Resumo
O campo linear elástico de tensões e deformações em torno de furos elípticos e entalhes semi-elípticos em placas de espessura finita é investigado por meio de análises 3D de elementos finitos. Significativas variações de fatores de concentração de tensão e deformação ao longo da espessura são identificados e comparados com soluções 2D. São analisados os gradientes de tensão nas vizinhanças da ponta do entalhe, e comparados com soluções 2D e resultados extraídos da literatura. Finalmente, considerações são feitas sobre impactos dos efeitos 3D sobre projeto de peças com entalhes.
Palavras chave: Entalhes tridimensionais; Concentração de tensão; Campos de tensão na ponta do entalhe; Efeitos da espessura.

[1] *Contribuição técnica ao 67º Congresso ABM - Internacional, 31 de julho a 3 de agosto de 2012, Rio de Janeiro, RJ, Brasil.*
[2] *Mechanical Engineer, Equipment Engineer, Petrobras.*
[3] *Mechanical Engineer, Ph.D., Professor Mechanical Eng. Dept., PUC-Rio.*
[4] *Civil Engineer, Ph.D., Professor Civil Eng. Dept., PUC-Rio*

ISSN 1516-392X

1 INTRODUCTION

The first remarkable solution for stress/strain fields around notches was obtained by Kirsch in 1898, for an infinite plate with a circular hole. Inglis in 1913 solved the infinite plate with an elliptical hole problem. Since then, a few analytical and many numerical and experimental solutions for other notch geometries have been proposed, but most of them treat the notches as if they could be properly described by a two-dimensional (2D) approximation. Peterson[1] provides a widely used catalog of stress concentration factors (SCF), although mostly restricted to plane and axisymmetric solutions. Creager and Paris[2] proposed a method to approximate notch SCF from the stress intensity factors (SIF) of similar cracks, but most listed SIF are 2D too.

It is well known, though, that stress/strain field perturbations close to notch tips are not restricted to in-plane components. In fact, due to Poisson's ratio, most notch tips assume a tri-dimensional (3D) stress/strain state. Youngdahl and Sternberg[3] and Sadowsky and Sternberg[4] solved the infinite solid with a 3D ellipsoidal cavity problem and obtained approximate solutions for the 3D stresses in an infinite plate of finite thickness with a circular hole. Through extensive finite element (FE) modeling of various notch configurations,[5-7] investigated 3D elastic fields on notched finite thickness plates under tension, coming to important conclusions, resumed as follows. If the x axis is aligned to the notch, y is perpendicular to the notch plane, and z is aligned to the notch front (Figure 1), then:

- the SCF of 3D notches depends on their thickness to tip ratio B/ρ and on their configuration;
- the $\sigma_{yy}(x)$ stress distribution along the notch mid-plane, normalized by the stress σ_{yy0} at the notch root, is almost insensitive to the plate thickness, and can be well approximated by the notch 2D solution;
- the mid-plane $\sigma_{yy}(x)/\sigma_{yy0}$ distribution is almost insensitive to the notch configuration up to $x/\rho \cong 0.75$, and is well approximated by Kirsch's plate and Creager-Paris' blunt crack solutions;
- although σ_{yy0} may vary significantly along the notch front, the $\sigma_{yy}(x)/\sigma_{yy0} \times x/\rho$ behavior is almost z-independent;
- the 3D affected zone is somewhat independent of the notch configuration for notches with opening angles lower than 90°, and is approximately 3/8 of the plate thickness.
- unlike crack problems, no matter how thick the plate is, it never reaches the plane strain condition, due to the finite notch tip radius;
- the out-of-plain constraint parameter $T_z = \sigma_{zz}/(\sigma_{xx} + \sigma_{yy})$ in the mid plane (T_{zmp}) variation along x/ρ is almost insensitive to plate thickness and notch configuration;
- $T_z/T_{z0}(x/B)$ is well approximated from FE results by equation (1)

$$T_{z0}/T_{z0mp} = 1 - 4.35(1 + 0.686\,x/B)^{-2} + 4.35(1 + 0.686\,x/B)^{-4} \quad (1)$$

- the through-thickness variation of $T_{z0}(z)/T_{z0mp}$ is nearly independent of the notch configuration; T_{z0} is maximal at the mid-plane and decreases to zero close to the free surface;
- the in-plain constraint factor $T_x = \sigma_{xx}/\sigma_{yy}$ around the notch tip, is nearly insensitive to the notch configuration and to the plate thickness, and can be approximated from Kirsch Plate or blunt crack solutions for the in-plane stress components.

Yang et al.,[8] presenting similar results, showed that stress and strain concentrations are decoupled along thickness even within the linear elastic (LE) regime. In-

ISSN 1516-392X

stead of the single 2D SCF $K_T = \sigma_{max}/\sigma_n = \varepsilon_{max}/\varepsilon_n$, independent K_σ and K_ε factors must be used in 3D notch problems.

In the present work, the 3D problems of an elliptical hole in an infinite plate and of a semi-elliptical notch in a semi-infinite plate are reviewed in the light of the observations of recent literature through LE FE analyses, and errors committed by simplified 2D modeling are briefly discussed.

2 METHODOLOGY

The software Abaqus 6.10-1 was used in the numerical modeling process. Several elliptical and semi-elliptical in finite thickness plates were built using C3D20 full integration solid element from Abaqus library. The following parameters were used:

Table 1: Finite Element Models parameters

Parameter	Symbol	Value
Poisson's ratio	ν	0.33
Elasticity Modulus	E	200GPa
Ellipsis horizontal axis	a	1mm
Ellipsis vertical axis	b	0.1mm to 1mm
Width	W	20mm (elliptical hole) 60mm (semi-elliptical notch)
Heigth	H	60mm
Thickness	B	

Plate width values were chosen to avoid boundary effects within 1% error, to properly approximate Inglis plate and a semi-elliptical notch in a semi-infinite plate. Every model was built with symmetry with respect to the *xy* plane at the plate mid-thickness and to the *xz* plane. The elliptical hole models received additional symmetry with respect to *yz* plane. The uniform load was applied as negative unitary pressure on the superior plate face ($y = H$). The meshing process followed some common guidelines. The notch tip region was mapped-meshed (Figure 1), with a maximum element size of $0.1 \cdot \rho$ at the notch tip. At a certain distance from the notch tip, the number of elements through thickness was reduced in order to save computational effort. The resulting linear equation systems were solved using Abaqus sparse solver.

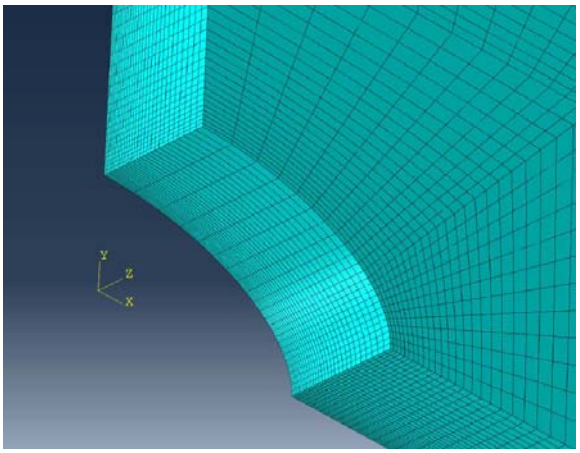

Figure 1: Finite element model.

ISSN 1516-392X

3 RESULTS

3.1 Stress and Strain Concentration along the Notch Tips

Figures 2 and 3 show the through-thickness variation of K_σ and K_ε obtained for an elliptical hole with *a/b = 0.5* for several thicknesses, and corroborate Yang's observation that K_σ and K_ε are different along the notch root thickness.[8]

Figure 4 shows the variation of their maxima values $K_{\sigma max}$ and $K_{\varepsilon max}$ with B/ρ, while Figure 5 shows the distance from the mid-plain where they act. Note how different such values can be (up to 15% for the analyzed models) and how their positions are slightly dissociated. Figure 6 shows $K_{\sigma mp}$, $K_{\sigma max}$, and $K_{\sigma surf}$ for the elliptical hole for increasing B/ρ ratios, where $K_{\sigma mp}$ and $K_{\sigma surf}$ are the SCF at the notched plates mid plane and surface. It synthesizes much of what has been recently published in the literature.

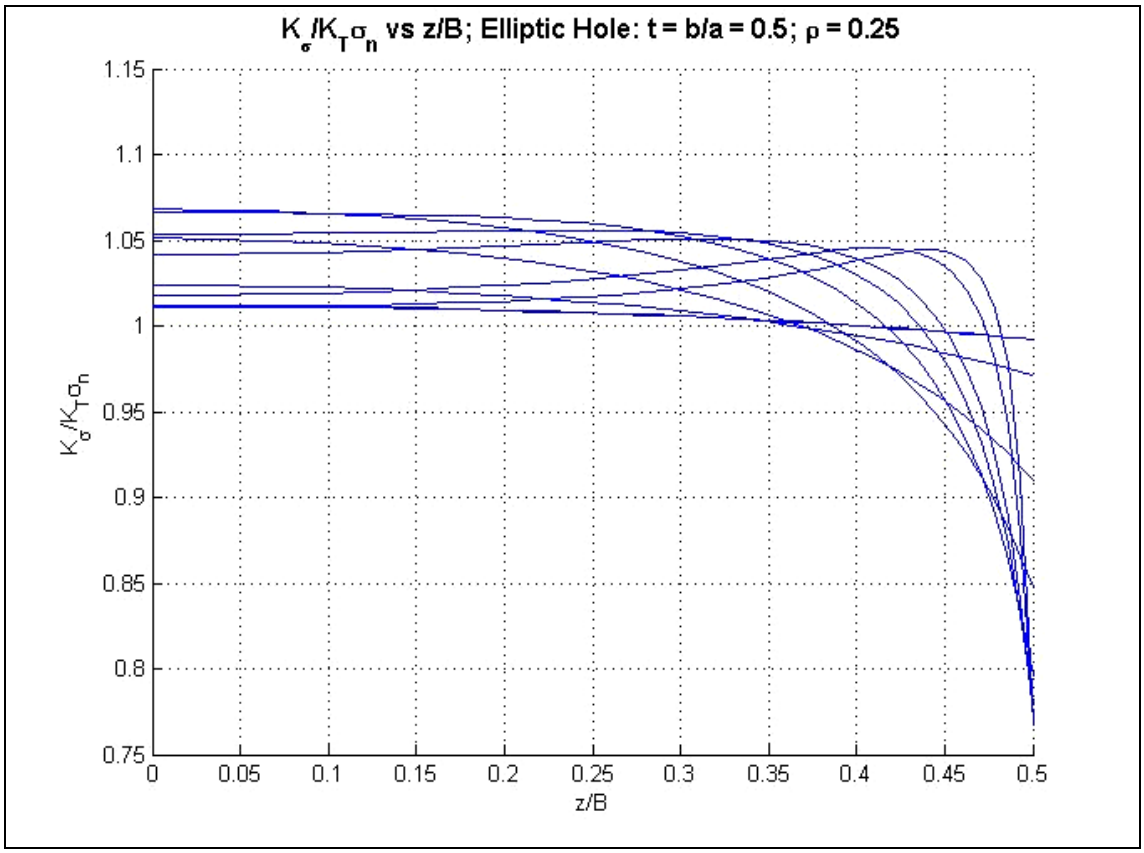

Figure 2: Through-thickness distribution of stress concentration factor.

As observed in Guo, Li e Kuang[5], and Guo and Li,[6] the ratio $K_{\sigma surf}/K_t$ is a monotonic decreasing function, which tends to unity if B/ρ is small (close to plane stress solution) and decays to an asymptotic value after some B/ρ ratio. In the interior of the plate, it is observed that $K_{\sigma max}$ and $K_{\sigma mp}$ are always higher then the plane solution prediction. These results show that $K_{\sigma max}$ occurs at mid plane for thin plates, but is attracted to the vicinity of the free surface, confirming what was observed in Guo, Li e Kuang[5] and Yang et al.[8] $K_{\sigma mp}$ tends to K_t for a very thin or for a very thick plate, while $K_{\sigma max}$ stabilizes at a constant value higher than K_t. It can also be seen that the sharper the tip radius, the wider the B/ρ transition band from a thin plate to a "saturated" thick plate, and the higher are the differences between K_σ and the plane K_t value.

ISSN 1516-392X

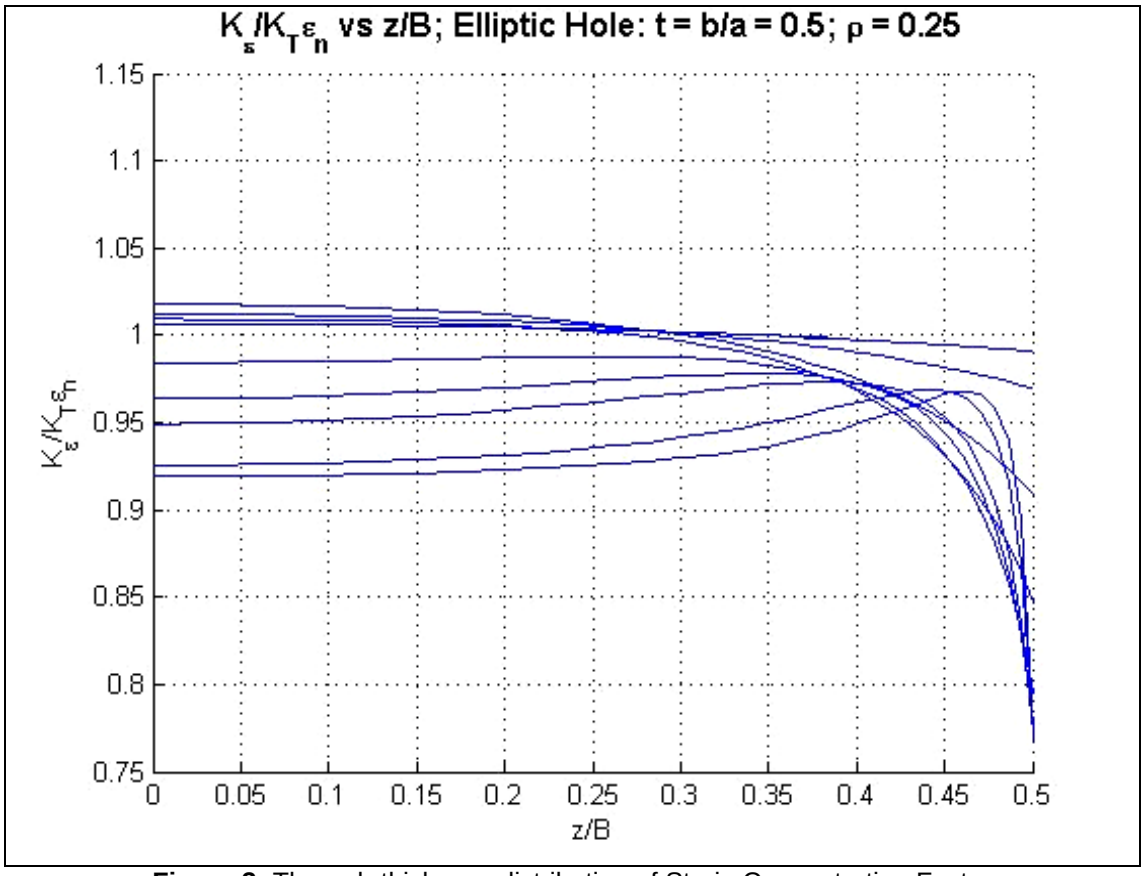

Figure 3: Through-thickness distribution of Strain Concentration Factor

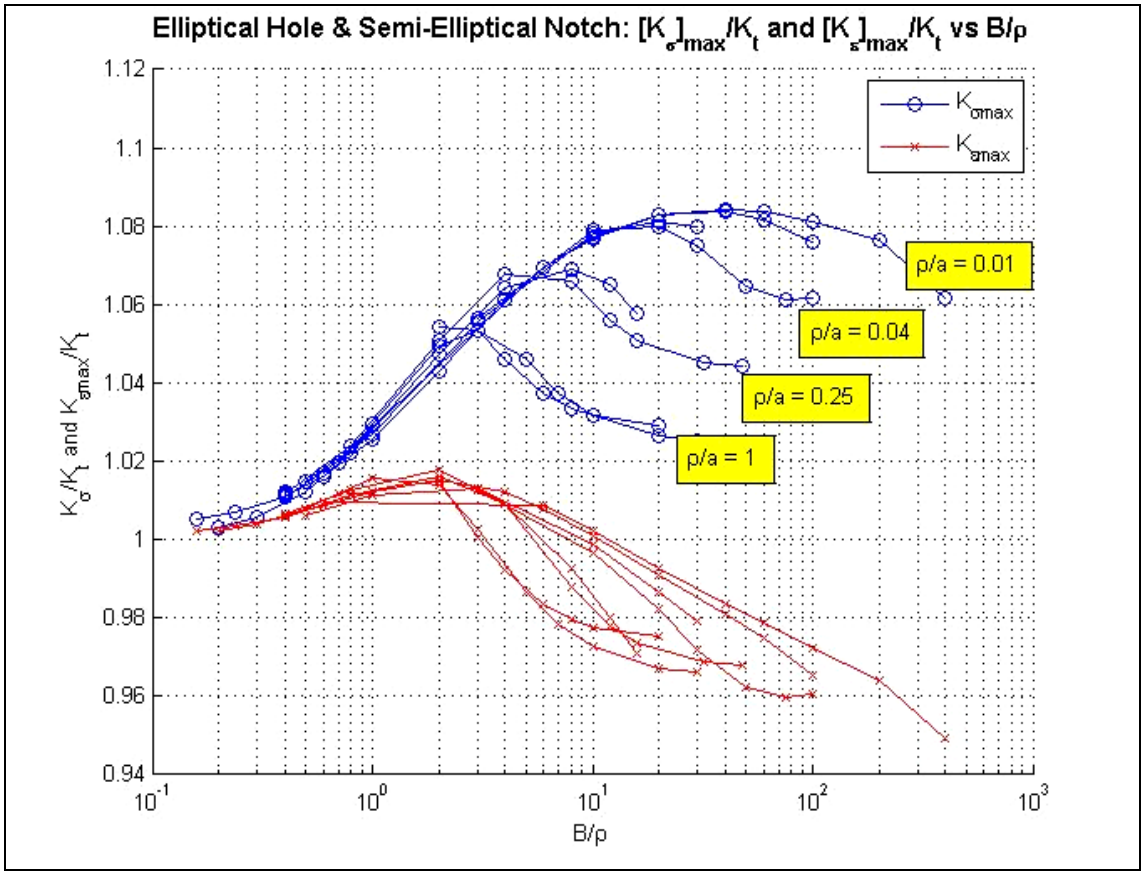

Figure 4: Maxima Stress and Strain Concentration Factors variation with normalized thickness.

ISSN 1516-392X

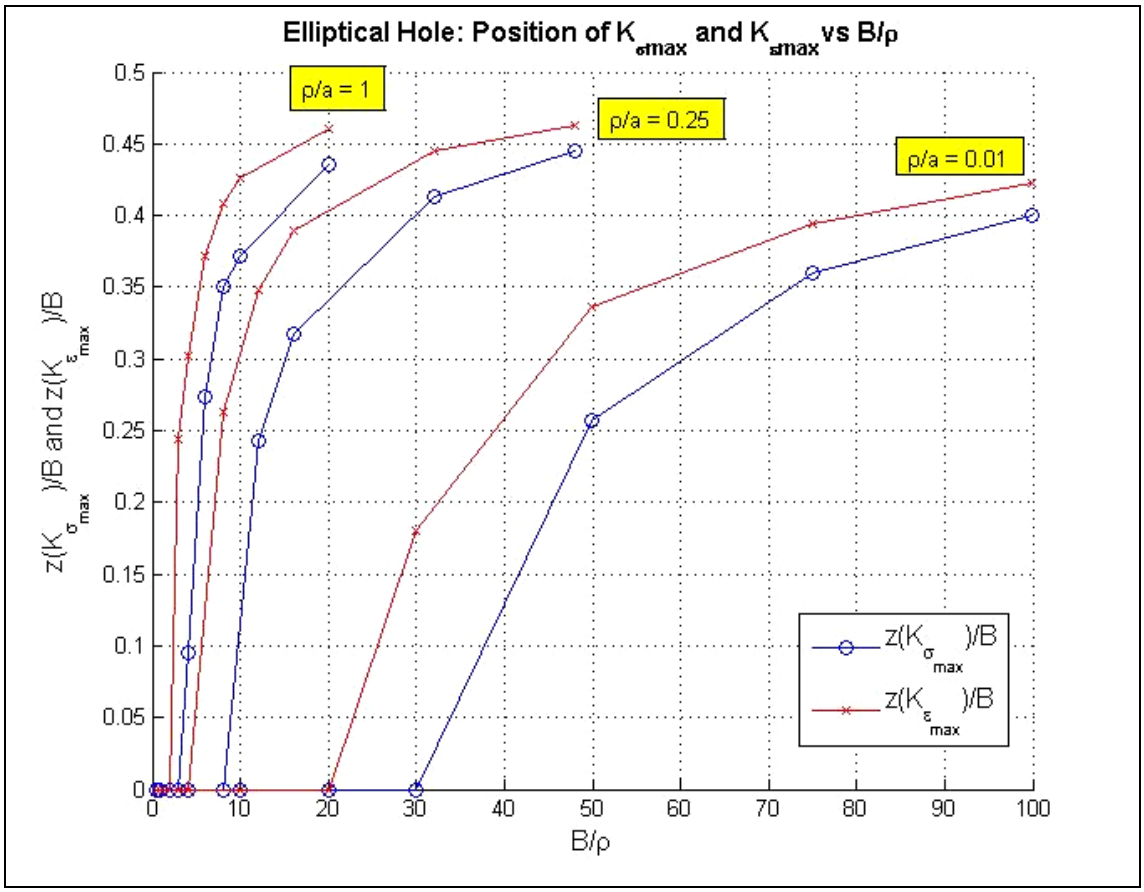

Figure 5: Position of Maximal Stress and Strain Concentration Factors along the notch root thickness.

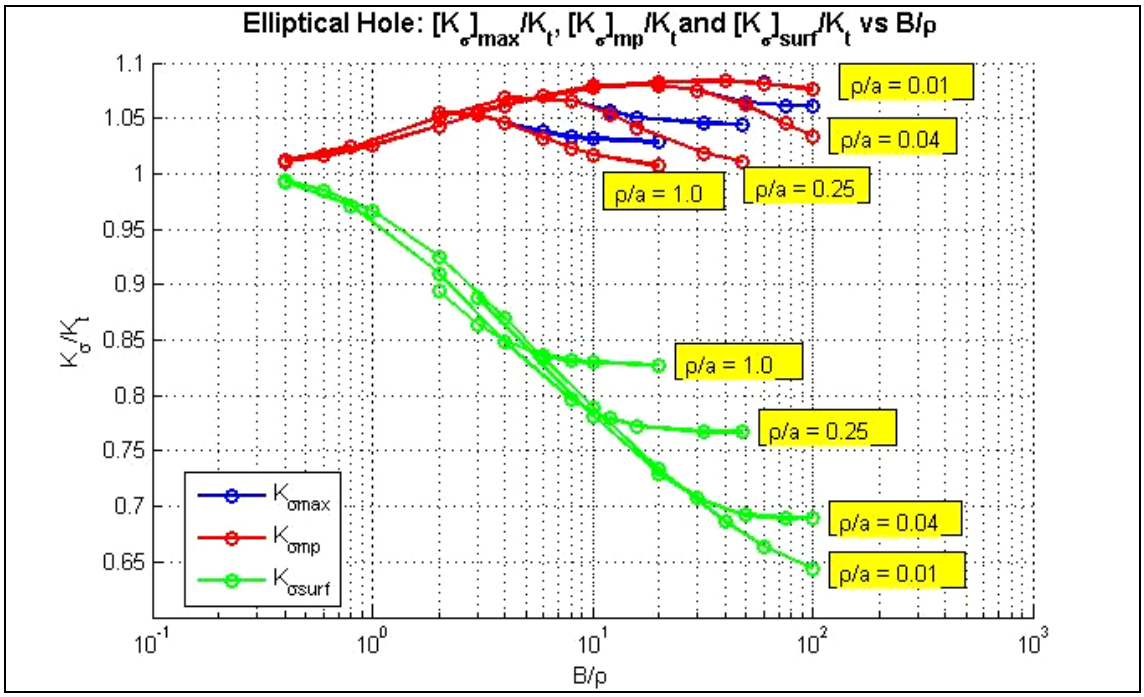

Figure 6: Stress Concentration Factor vs. thickness: at free-surface, at mid-plane and maximal.

Figure 7 shows the $\sigma_{yymp}(x)/\sigma_{yy0mp}$ profile along x/ρ in the vicinity of the notch tip for all analyzed elliptical holes and semi-elliptical notches. As mentioned before, up to $x/\rho \cong 0.75$ the stress profile is nearly independent of the notch tip radius, the thick-

ISSN 1516-392X

ness and the notch shape itself. Also, the approximated 2D solutions of Kirsch plate and Creager-Paris are very good approximations for $\sigma_{yymp}(x)/\sigma_{yy0mp}$.

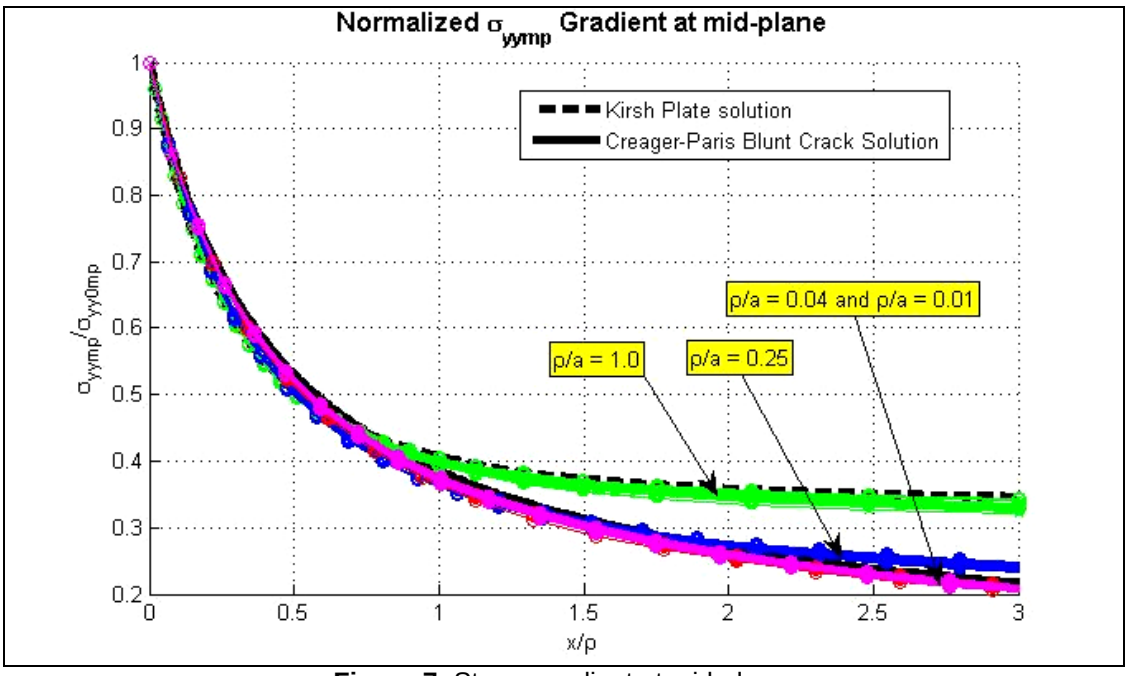

Figure 7: Stress gradient at mid-plane.

Figure 8 shows that, for several *z*-planes along the plate thickness, the $\sigma_{yy}(x)/\sigma_{yy0}$ ratio behaves similarly. In other words, even if K_σ presents through-thickness variation, the σ_{yy} stress gradient along x/ρ close to the notch tip can be well predicted by the 2D solution.

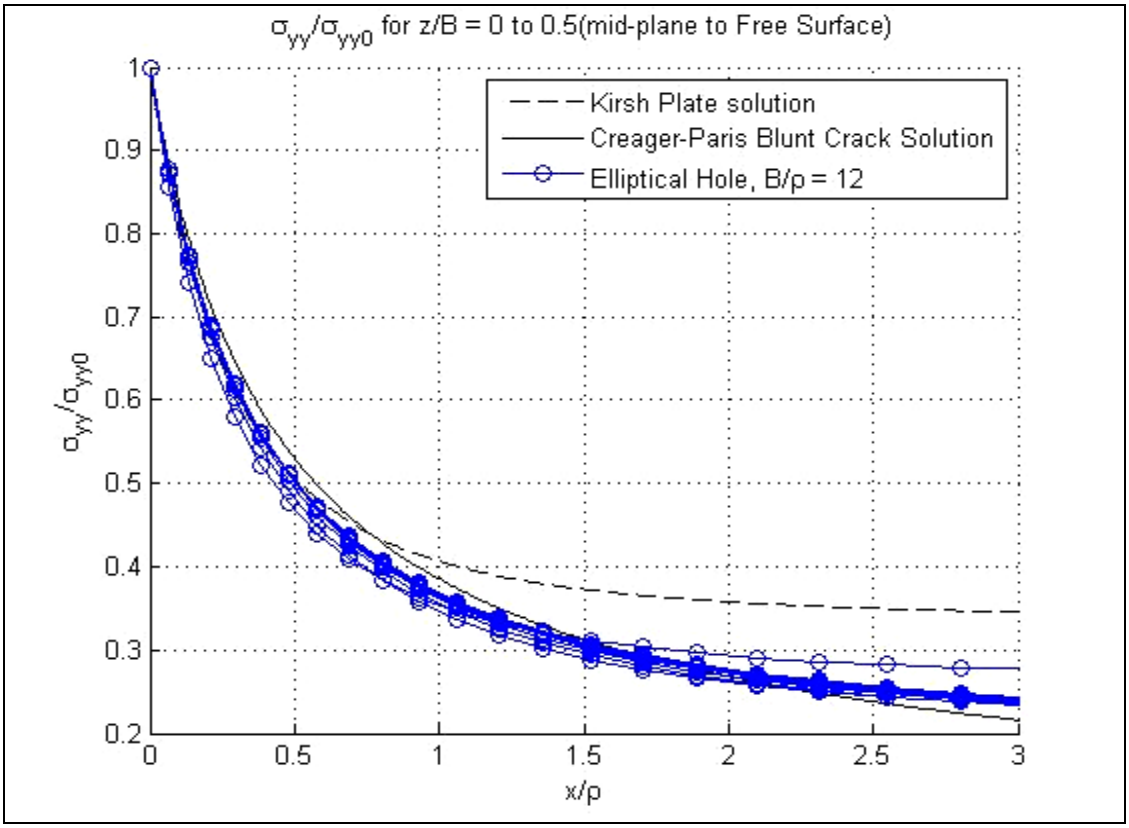

Figure 8: Stress gradient at several *z*'s.

ISSN 1516-392X

3.2 In-plain Constraint Factor

The in-plain constraint factor $T_x = \sigma_{xx}/\sigma_{yy}$ along x/ρ in the mid-plane is shown in Figure 9. It can be seen that the T_x dependency on the notch shape and thickness decreases close to the notch tip. At $x/\rho = 0.3$ it is within a 0.05 range (approximately 20% error), and Kirsch and Creager-Paris solutions are good lower and upper-bound approximations, as affirmed by Guo, Li e Kuang.[5]

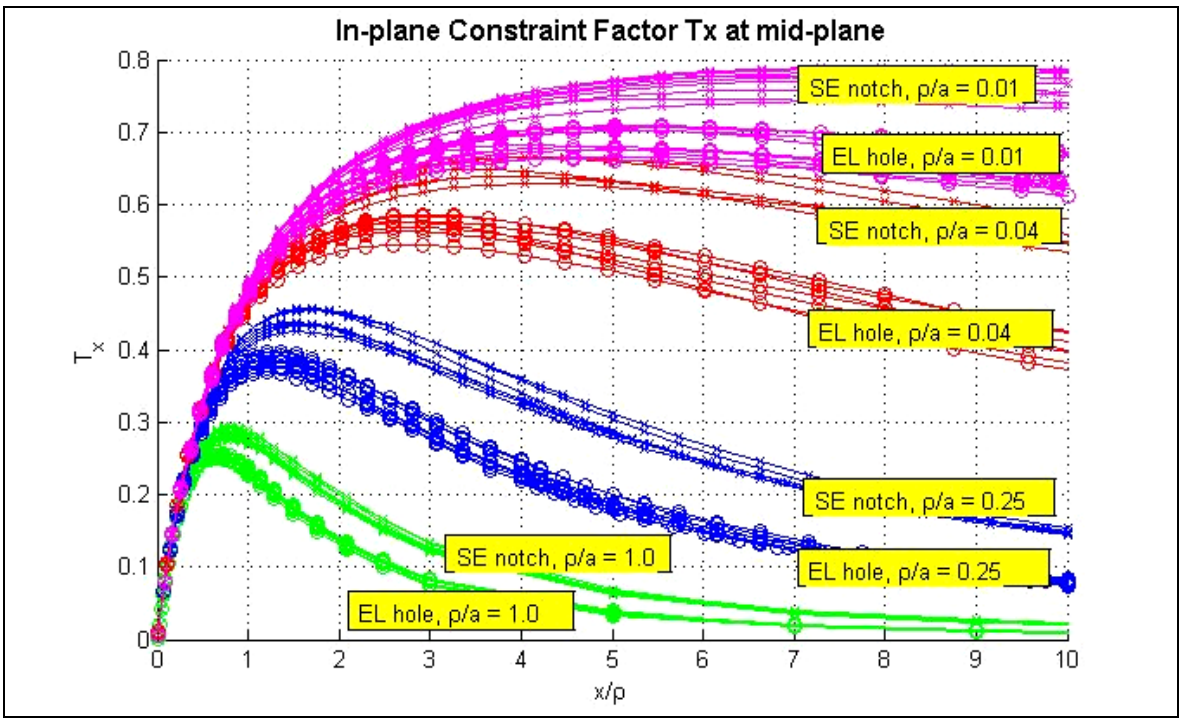

Figure 9: In-plane constraint along x/ρ.

3.3 Out-of-plane Constraint Factor

Figure 10 shows the the increase of T_{z0mp} with the plate thickness. It can be seen that, indeed, the out of plane constraint factor T_z in the interior of the plate reaches a saturated value, which becomes closer to Poisson's ratio for sharper notch tip radii.

Figure 11 shows T_{zmp}/T_{z0mp}, and the expression fitted by Guo, Li e Kuang.[5] As it can be seen, the present results show good agreement with Guo's results for x/B below 0.4, and shows that no out-of-plain restriction is expected at a distance B from the notch tip.

4 IMPLICATIONS ON NOTCHED PIECES DESIGN

It is important to verify the influence of the studied notch tip stress/strain fields in the main failure criteria employed in structural components design. For example, Tresca (maximum shear stress) and Mises (maximum distortion energy) equivalent stresses can be expressed by:

$$\sigma_{Tresca} = \sigma_{11} - \sigma_{33} \tag{2}$$

$$\sigma_{Mises} = \sqrt{0.5\left[(\sigma_{11} - \sigma_{22})^2 + (\sigma_{22} - \sigma_{33})^2 + (\sigma_{33} - \sigma_{11})^2\right]} \tag{3}$$

ISSN 1516-392X

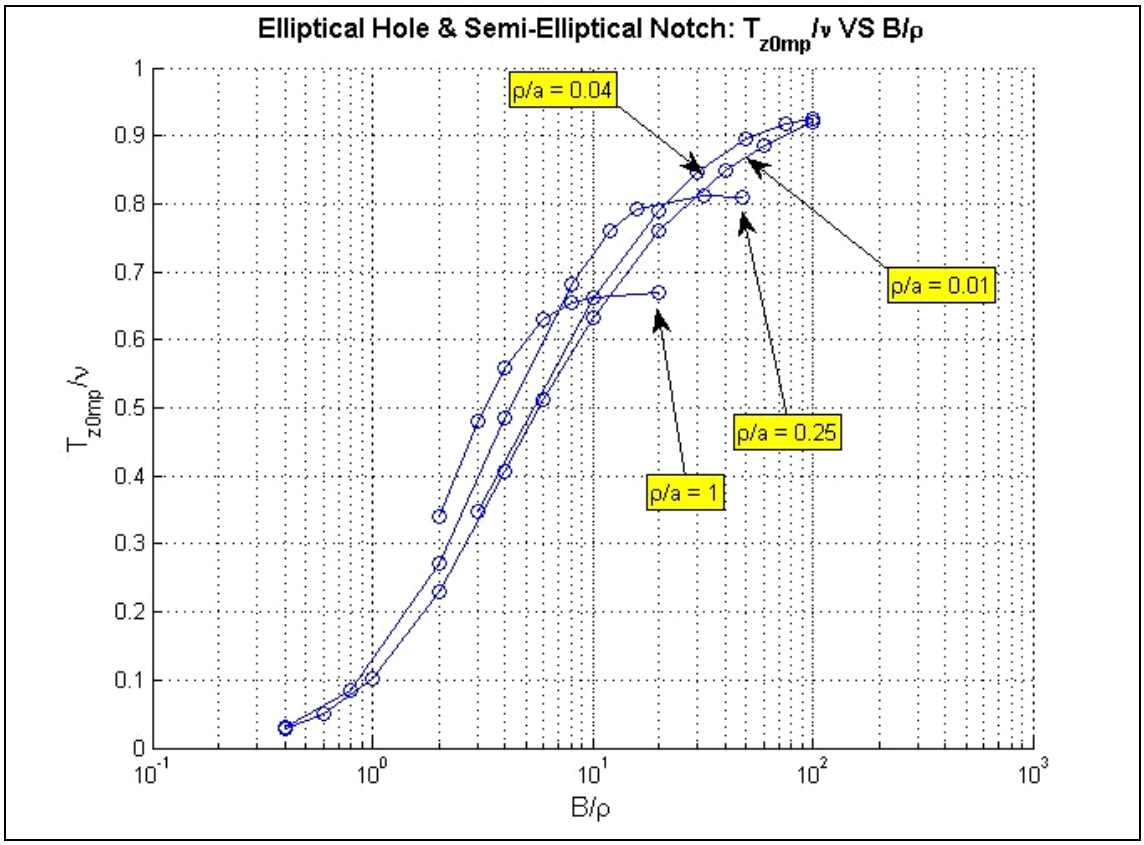

Figure 10: Out-of-plane constraint factor T_z at mid-plane with thickness

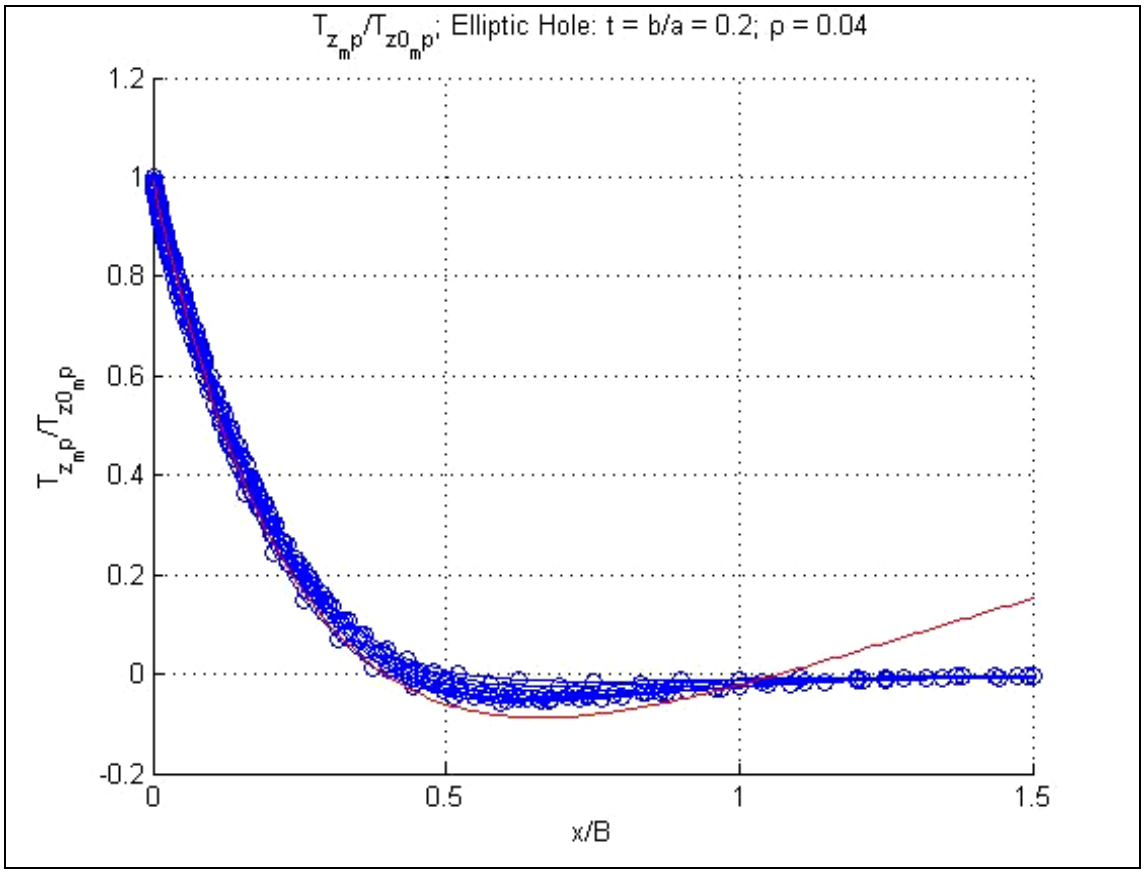

Figure 11: Out-of-plane constraint T_z ahead of the notch tip

ISSN 1516-392X

It is known that along the notch root, the only non-null stress components are σ_{yy} and σ_{zz}, and that they are both tensile in the scope of this work. Therefore, principal stress components will be σ_{yy} and σ_{zz}. Using the out-of plane constraint factor T_z previously defined, σ_{zz} can be rewritten as:

$$\sigma_{zz} = T_z \sigma_{yy} \tag{4}$$

Tresca's equivalent stress becomes simply σ_{yy} and σ_{Mises} can be expressed by:

$$\sigma_{Mises} = \sigma_{yy} \sqrt{1 - T_z + T_z^2} \tag{5}$$

From the above expression, it can be observed that T_z decreases σ_{Mises}, which is reasonable, as the out-of-plain constraint should prevent distortion. Let us assume, for instance, that σ_{yy0} at the notch root was calculated from a 2D solution (simply $\sigma_{yy0\_2D} = K_{T\sigma n}$), and therefore contains an intrinsic error with respect to 3D solution. In the notch tip, errors in Tresca and Mises equivalent stresses could be written as:

$$1 + err_{Tresca} = \sigma_{yy0} / K_t \sigma_n \tag{6}$$

$$1 + err_{Mises} = \sigma_{Mises} / K_t \sigma_n \tag{7}$$

The results presented in the previous sections show that σ_{yy0} will always be higher when thickness effect is accounted for, meaning that 2D predictions are non-conservative. As for Mises, Figure 12 shows $\sigma_{Mises}/K_T\sigma_n$ for several arbitrary values of error on σ_{yy0} when calculated from 2D plane solutions.

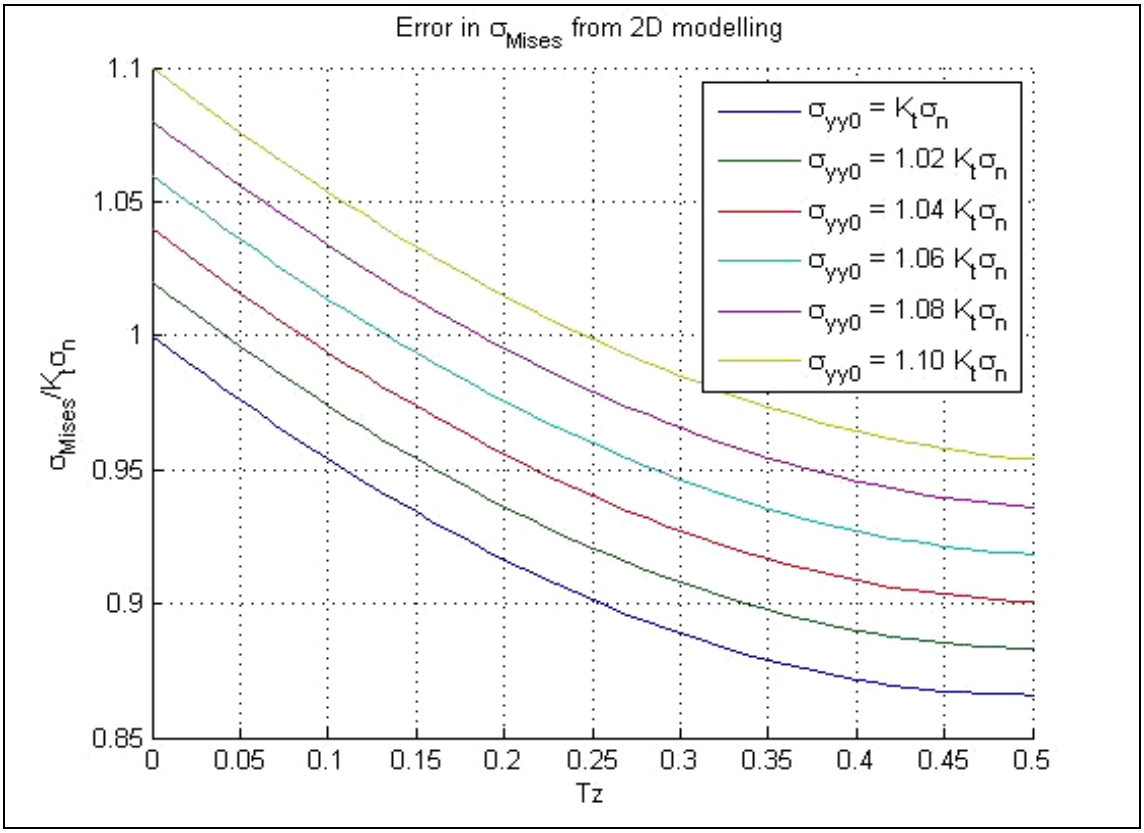

Figure 12: Error in Mises equivalent stress from 2D modeling

ISSN 1516-392X

From previous discussion, it is known that Poisson's ratio is an upper bound limit to T_z, and Guo, Li e Kuang[5] shows that this limit is in fact never reached for a finite notch tip radius, no matter how thick the plate is. Also, Guo et al.[9] shows that $(K_{\sigma max}/K_T)_{peak}$ for an Elliptical Hole in an infinite plate is a function of ν and the aspect ratio t of the Elliptic Hole, fit with the curve:

$$K_{\sigma max}/K_t = 1 + 0.01\exp[\nu/(0.14364 + 0.07t)] \quad (8)$$

Inglis proposes that the K_t of any notch of depth a and tip radius ρ can be estimated as an equivalent elliptic hole through the formula:

$$K_t = 1 + 2\sqrt{a/\rho} \quad (9)$$

If assumed that expression (7) is applicable for any defect, regarded that the defect has the same depth a and tip radius ρ, $(K_{\sigma max}/K_T)_{peak}$ can be expressed in terms of K_T itself:

$$(K_{\sigma max}/K_t)_{peak} = 1 + 0.01\exp[\nu/(0.14364 + 0.14/(K_t - 1)] \quad (10)$$

Figure 13 illustrates the adapted expression for most common Poisson's ratios used in engineering structure materials. The validity of the above predictions is questionable for K_T values way above 3, if the notch is expected to work under tension and remain in elastic regime. That means that, in design terms, 8% is a good assumption for upper bound limit for $K_{\sigma max}$ and, consequently, for Tresca criterion.

With respect to Mises equivalent stresses, Figure 12 shows that the 2D prediction is non-conservative for a combination of low K_T and relatively high $K_{\sigma max}/K_T$. These two requisites are, in fact, competitive, as T_z decreases for thin plates and non-sharp notches, where $K_{\sigma max}/K_T$ tends to be low too. These considerations suggest that σ_{Mises} should be conservatively predicted by 2D solutions in most cases.

Figure 14 shows $K_{\sigma max}/K_T$ and $\sigma_{Mises}/K_T\sigma_n$ of the present results, illustrating the error committed in 2D modeling, when 3D effects are not accounted. As expected, maximum 2D modeling error was around 8% non-conservative for σ_{yy0}, while σ_{Mises} 2D predictions presented no significantly unsafe error (below 1%).

5 CONCLUSIONS

Several 3D finite element analyses were performed in order to obtain the elastic fields ahead of elliptic holes and semi-elliptical notches in finite-thickness plates. Stress and strain concentration factors were observed along the notch root thickness, and presented substantial difference (more than 5%) for $x/\rho > 2$.

Stress concentration distribution along the notch root thickness was shown to be minimal at the free surface. The maximum stress concentration is achieved in the interior of the plate, at the mid-plane for a relatively thin plate, or close to the free surface for a thick plate.

σ_{Mises} gradient ahead of the notch root was shown to be well represented by the 2D solution, and well approximated be Kirsch or Creager-Paris solutions in the vicinity of the notch root.

ISSN 1516-392X

It was observed that the maximal T_z in the notch root increases with the plate thickness, but saturates in a value below Poisson's ratio. Also, it was shown that T_z fades at $x/B = 1$.

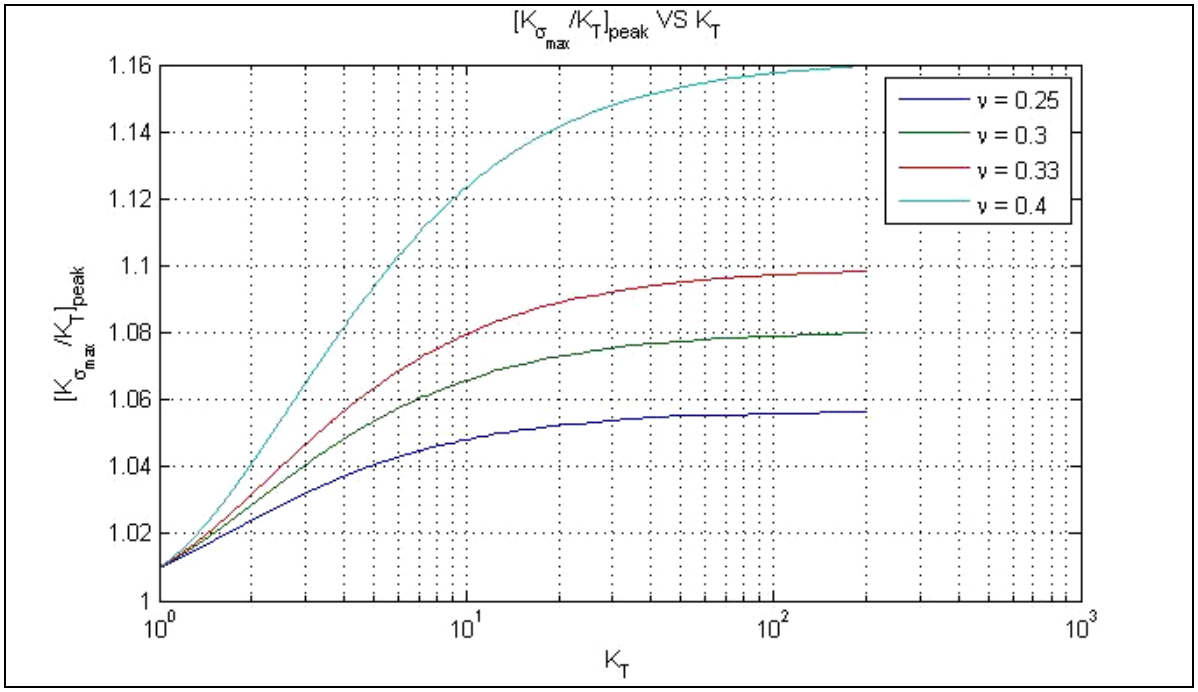

Figure 13: Estimated error $(K_{\sigma max}/K_T)_{peak}$ in 2D calculation.

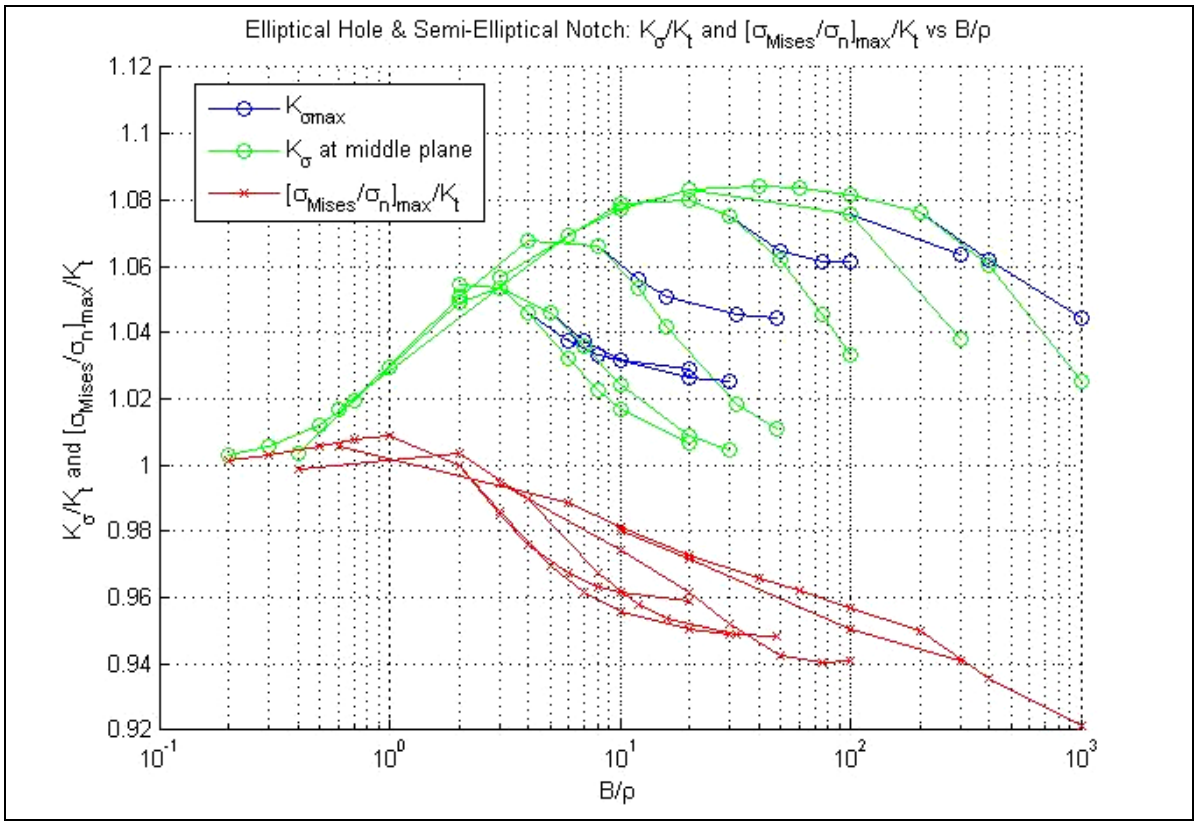

Figure 14: $K_{\sigma max}/K_T$ and $\sigma_{Mises}/K_T\sigma_n$ in the present work

Based on present results and data provided in literature, it was shown that Tresca's equivalent stress prediction from 2D modeling is always non-conservative, while

ISSN 1516-392X

Mises equivalent stress 2D prediction is conservative in most cases. Also, if the specimen is designed to work within elastic limits, errors in 2D associated with 3D effects above 8% are not expected.

Acknolodgements

Dr. Alexandre Hansen from PETROBRAS provided considerable assistance on the Finite Element software. CNPq provided scholarships for the senior authors.

REFERENCES

1 PETERSON's Stress Concentration Factor, John Wiley & Sons, 2008.
2 CREAGER, M.; PARIS, P.C. Elastic field equations for blunt cracks with reference to stress corrosion cracking. Int. J. Fatigue 3, 247-252, 1967.
3 YOUNGDAHL, C.K.; STERNBERG, E. Stress Concentration around a triaxial ellipsoidal cavity. Journal of Applied Mechanics p. 149-157, 1949.
4 SADOWSKY, M.A.; STERNBERG, E. Three-Dimensional Stress Concentration Around a Cylindrical Hole in a Semi-infinite Body. Journal of Applied Mechanics p. 855-864, dec. 1966.
5 GUO, W., LI, Z., KUANG; Three-dimensional elastic stress fields near notches in finite thickness plates. Int. J. Solids and Structures 37, 7617-7631, 2000.
6 GUO, W., LI, Z.; Three-dimensional elastic stress fields ahead of blunt V-notches in finite thickness plates. Int. J. Fracture 107, 53-71, 2001.
7 GUO, W., SHE, C.; Three-dimensional stress concentrations at elliptic holes in elastic isotropic plates subjected to tensile stress, Int. J. Fatigue 29, 330-335, 2007.
8 YANG, Z.; KIM, C.B, CHO, C., BEOM, H.G.; The concentration of stress and strain in finite thickness elastic plate containing a circular hole. Int. J. Solids and Structures 45, 713-731, 2008.
9 GUO, W.; YU, P., SHE, C., ZHAO, J.; The influence of Poisson's ratio on thickness-dependent stress concentration at elliptic holes in elastic plates. Int. J Fatigue 30, 165-171, 2008.